MnO_x - Promoted, Coking-Resistant Nickel-based Catalysts for Microwave-initiated CO_2 Utilization

Weisong Li[1,2†], Xiangyu Jie[2†], Changzhen Wang[3], Jonathan R. Dilworth[2], Chunjian Xu[1*], Tiancun Xiao[2*]and Peter P. Edwards[2*]

[1]School of Chemical Engineering & Technology, State Key Laboratory of Chemical Engineering, Tianjin University, Tianjin 300350, China

[2]Inorganic Chemistry Laboratory, University of Oxford, South Parks Road, Oxford OX1 3QR, UK

[3]Engineering Research Center of Ministry of Education for Fine Chemicals, Shanxi University, Taiyuan 030006, China

† Authors contributed equally

Corresponding authors: Peter P. Edwards (peter.edwards@chem.ox.ac.uk); Tiancun Xiao (xiao.tiancun@chem.ox.ac.uk) and Chunjian Xu (cjxu@tju.edu.cn)

Abstract

The most important factors in improving the stability of nickel-based catalysts for methane reforming with carbon dioxide (so-called methane dry reforming, MDR) lie both in suppressing carbon formation and inhibiting metal sintering at the high operating temperatures of this process (typically above 700 °C). Many efforts had been made to overcome these challenges, for example, by enhancing metal catalyst-support interactions. In this work, we used microwaves as an energy source to drive the MDR reactions under mild conditions with an overall measured catalyst bed temperature of below 220˚C. High CH_4 conversion of ca. 94% and 97% conversion of CO_2 were achieved over manganese-oxide modified ZrO_2-supported nickel catalysts, exhibiting excellent anti-coking properties. Compared with Ni/ZrO_2 and Mn/ZrO_2 catalysts, the Ni-Mn bimetal catalytic system stabilizes the catalytic activity of MDR by suppressing carbon deposition with the mixed-valent Mn^{3+}/Mn^{2+} chemical states enhancing the absorption and conversion of CO_2 during the reactions.

1. Introduction

The atmospheric concentration of CO_2 has increased from 280 ppm in the pre-industrial age to more than 400 ppm now and is expected to be above 500 ppm by the end of this century.[1] To solve the challenge of global warming, technologies such as CO_2 capture and storage (CCS), renewables and end-use energy efficiency improvement are actively proposed to reduce 82% of the global CO_2 emissions by 2050.[2-3] However, current CCS remains costly and the potential ecological hazards associated with underground CO_2 sequestration are still uncertain.[4] Alternatively, CO_2 is now recognized as an important carbon source for chemical production and recent work has reported utilising CO_2 to produce fuels and chemicals,[5-7] involving electro or photocatalytic reduction.[8-10] Compared to these lab-scale technologies which are still far from industrial applications, the reforming of methane with CO_2 into syngas (H_2 and CO mixture) is now operating close to commercial viability in different parts of the world. Additionally, the obtained syngas could then be used as feedstock for the chemical synthesis to produce liquid hydrocarbon fuels, olefins and alcohols, etc.

Nickel-based catalysts have been widely used in methane dry reforming (MDR) because of their comparable activity to noble metals at a relatively modest cost.[11] However, the difficulties which accompany their industrial application are severe carbon deposition and inevitable Ni catalyst sintering when operating at high process temperatures.[12-14] In order to resolve these challenges, methods such as the control of particle sizes, particles-confinement and constructing core-shell structures have been studied.[13] However, the preparation of core-shell capsule catalysts is highly complex and thus simple strategies by adding promoters such as Mn[15-17] and Mg[18-19] etc. had been advanced and noticeably improved the anti-coking ability of the supported metal catalysts. Although considerable effort has been made towards metal size control and confinement, it is always difficult to prevent the metal sintering at high operating temperature of MDR (700–900 °C) initiated by Ostwald ripening.[13] Thus, it would be highly desirable to reduce the MDR operating

temperatures through alternative methods to improve both the catalyst stability and performance .

Microwave heating is an effective and fast approach to deliver energy directly to the reaction through localized hot-spots, rather than heating the entire catalyst bed by conventional thermal convection or conduction.[20] Normally, a temperature gradient is formed between the induced hot catalyst particles (microwave absorber/acceptor) and surroundings; thus, importantly, the bulk temperatures of the catalyst bed are therefore reduced. Due to the fundamentally different heating mechanism, microwave-assisted catalytic processes are found to offer high conversions and selectivities at relatively low/safe overall temperatures.[21-23] Over the past decade, many attempts have been made to reform methane with CO_2 under microwave irradiation.[24-28] Zhang et al. reported MDR using microwave dielectric heating over an Al_2O_3 supported platinum catalyst. They claimed, due to the formation of hot spots under microwave irradiation, higher conversion and selectivity were obtained under microwave conditions than those obtained with conventional thermal process when operating at the same measured temperature.[24] It should be noted also that typical supports used for the conventional thermal MDR such as Al_2O_3, ZrO_2 and SiO_2 or their modified forms[13, 29-32] are not suitable for the microwave-assisted processes due to the lack of microwave absorption. Therefore, the catalyst systems for microwave-assisted MDR are needed to modify by either mechanically mixing traditional catalysts with a microwave receptor such as active carbon or alternatively using high dielectric materials as supports for metal catalysts in order to enhance the overall microwave absorption.[33-35] As the prototypical dielectric materials, manganese oxides possess good microwave absorption properties[36] and their great potential in catalysis, especially in catalytic CO_2 utilization processes, have attracted growing interest.[37-39] In addition, due to the multivalent properties of manganese, manganese oxides could help induce active oxygen species to facilitate efficient oxidation or fast coke elimination in some hydrocarbons evolved reactions.[40,41] Naturally, therefore, manganese oxide appears to be an ideal promoter to supress carbon deposition and modify the nickel-based catalysts to be suitable for efficient and stable methane reforming with

CO_2 under microwave irradiation.

In this work, we developed a facile way to synthesize series of manganese oxide promoted nickel-based catalysts supported by ZrO_2 for microwave-assisted methane reforming with CO_2. Consequently, the Ni-Mn bimetal catalytic system could facilitate efficient and stable MDR reaction under microwave irradiation. Compared with the reference nickel catalyst which was synthesized under the same conditions, the carbon deposition on Ni-Mn/ZrO_2 catalysts was significantly suppressed, revealing that manganese oxides can help to improve the nickel-based catalyst to make it suitable for microwave-assisted methane dry reforming with significantly improved coking-resistant ability and process performance.

2. Experimental

2.1 Chemicals

Analytical grade nickel nitrate hexahydrate ($Ni(NO_3)_2 \cdot 6H_2O$), citric acid monohydrate ($C_6H_8O_7 \cdot H_2O$), zirconium oxide (ZrO_2) and manganese dioxide powder (MnO_2) were purchased from Sigma-Aldrich and used without further purification. Deionized water was used for the preparation of catalysts.

2.2 Catalysts preparation

Typically, 20 mmol MnO_2 powder and 24 mmol citric acid monohydrate were mixed with 30 mL deionized water. The mixture was then placed and stirred on a 100 °C magnetic hot plate to form a transparent dark yellow solution. Various ratios of $Ni(NO_3)_2 \cdot 6H_2O$ and ZrO_2 support were added to the solution to form an uniform suspension. A slurry was then formed by vigorous stirring and heating. Finally, the slurry was calcined in the 500 °C muffle furnace for 2 hours with a ramping rate of 5 °C/min. The as-prepared catalyst was collected and crushed into fine powder for use. For comparison purposes, a series of NiMn/ZrO_2 catalysts were prepared with different Ni/Mn ratios as summarised in Table 1.

Table1. Composition of each designed catalyst for methane reforming with CO_2

Catalysts	Molar ratios		
	Ni	Mn	ZrO_2
Ni/ZrO_2	1	0	2
Mn/ZrO_2	0	1	2
$NiMn/ZrO_2$-1	0.5	0.5	2
$NiMn/ZrO_2$-2	0.3	0.7	2
$NiMn/ZrO_2$-3	0.1	0.9	2
$NiMn/ZrO_2$-4	0.05	0.95	2
$NiMn/ZrO_2$-5	0.025	0.975	2
$NiMn/ZrO_2$-6	0.05	0.95	1
$NiMn/ZrO_2$-7	0.05	0.95	3

2.3 Microwave-assisted methane reforming with CO_2

The microwave-assisted MDR reaction was carried out in a custom-built single mode microwave reactor, and the schematic reaction flowsheet is illustrated in **Scheme 1**. Typically, 1.0 g of catalyst was loaded in a quartz tube reactor with an inner diameter of 8 mm. The tube reactor was placed into the cavity with the catalyst bed being located at the centre to ensure the uniform microwave irradiation and the temperature was recorded with an IR pyrometer.

The catalyst was directly activated in the methane reforming feedstock (47/47 vol.% CO_2/CH_4 mixture, balanced by Argon) flow under microwave irradiation. In the activation period, the feed flowrate was fixed at 100 mL/min and the catalysts were exposed to microwaves for 3 minutes with the microwave input power (P_I) being fixed at 200 W. After activation, the microwave was turned off and the reactor was cooled down to room temperature. Then, the gas flowrate was adjusted to the designed feed flowrate for the methane reforming reaction and the microwave input power was fixed at 100 W for the whole continuous methane reforming period. During the reforming period, the outlet gases were collected, and their compositions were analysed with a calibrated Perkin Elmer Clarus gas chromatography (GC) every 1 hour. To reduce the dissolution of CO_2 in water during the gas collection and storage in metrical cylinders, the pH of water was adjusted to 4 using diluted H_2SO_4 to ensure the accuracy of the gas compositions. In the microwave reaction, the control of microwave input power and the recording of the reflected microwave power (P_r) and

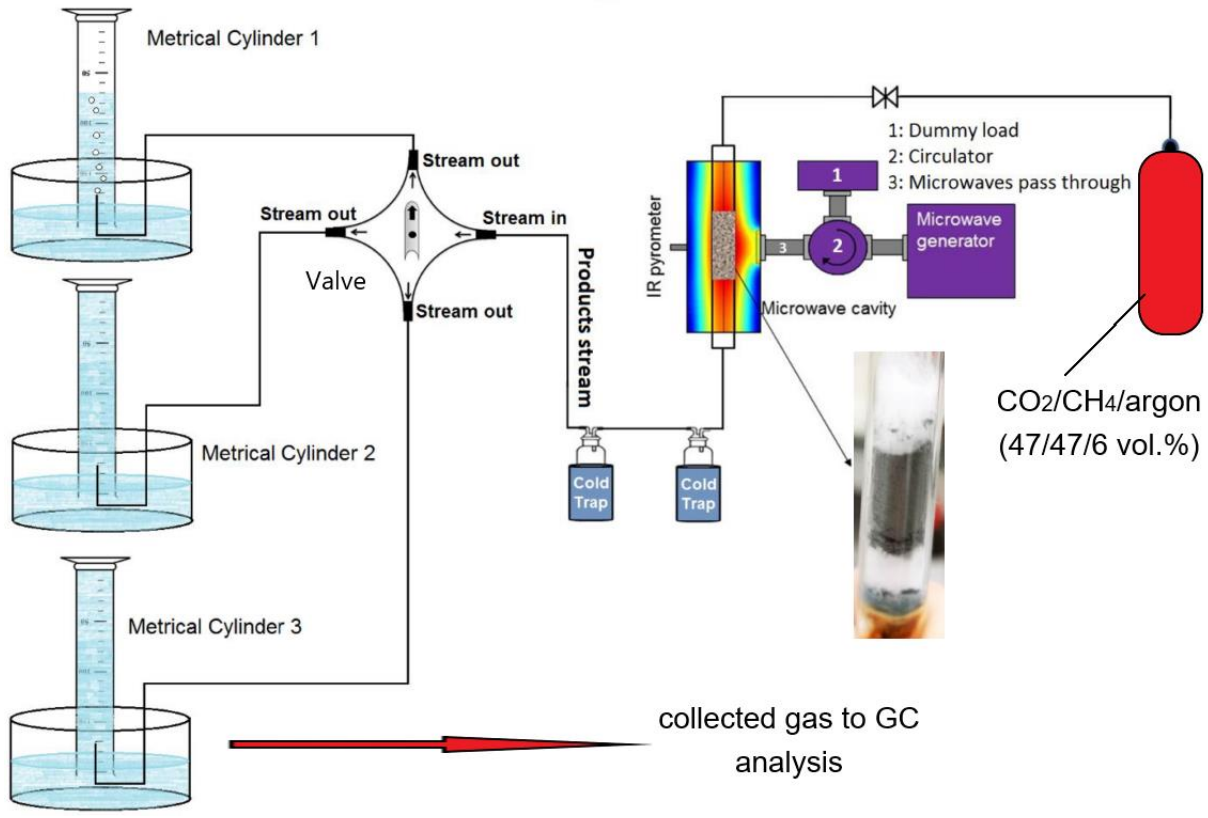
catalyst bed temperature were taken through the pre-installed Labview software. In this work, the absorbed microwave power (P_a) is defined as $P_a=P_I-P_r$.

Regarding to the conversions of CH_4 and CO_2, argon was used as internal standard for the conversion (X) calculations and they were calculated using the following equations:

$$X_{CH4} = (CH_{4\,(f)}-CH_{4\,(out)})/CH_{4\,(f)} = (R_{CH4\,(f)}-R_{CH4\,(out)})/R_{CH4\,(f)} \quad \text{(equation 1)}$$

$$X_{CO2} = (CO_{2(f)}-CO_{2\,(out)})/CO_{2\,(f)} = (R_{CO2\,(f)}-R_{CO2\,(out)})/R_{CO2\,(f)} \quad \text{(equation 2)}$$

Here, R represents the molar ratio of CH_4/argon or CO_2/argon and these ratios are obtained from the GC analysis data, the subscripts (f) and (out) represent the feedstock and outlet gas, respectively.



Scheme 1. Schematic configuration for the microwave-assisted reforming of methane with CO_2 (modified from *Angew. Chem. Int. Edit.* **2017**, *56*(34), 10170-10173.).

2.4 Sample characterization

The X-ray diffraction patterns of the samples were collected using a Bruker D8 Focus

Diffractometer with Cu Kα as the radiation source. The surface morphologies and elemental analysis of fresh and used samples were carefully studied by scanning electron microscope (SEM) and energy dispersive X-ray spectroscopies (EDS) using a ZEISS EVO. X-ray photoelectron spectroscopy (XPS) was performed on an ESCALAB 250XI (Thermal Scientific, USA) X-ray photoelectron spectrometer. The amount of carbon deposition on the catalysts was quantified by a thermogravimetric analyser (TGA, SDT-Q600, TA instrument, USA) under 100 mL/min air flow with a ramping rate of 10 ˚C/min.

3. Results and Discussion

3.1 Methane reforming performances over catalysts having different compositions

The microwave-assisted reforming reactions over catalysts with different compositions were carried out with a total feed flowrate of 2000 mL/h. As a general observation, manganese oxide modified nickel catalysts ($NiMn/ZrO_2$) showed much better stability than those of Ni/ZrO_2 and Mn/ZrO_2 catalysts (**Figure 1**). The $NiMn/ZrO_2$-4 and $NiMn/ZrO_2$-5 catalysts revealed a very stable CH_4 conversion at around 94% over 10 hours reaction, whereas the CH_4 conversion of Ni/ZrO_2 and Mn/ZrO_2 catalysts dropped drastically to 53.3% and 74%, respectively, after 10 hours' reaction (**Figure 1A**). It is also noted that, the stability of CH_4 conversion over the $NiMn/ZrO_2$ catalysts were increased by decreasing the Ni/Mn molar ratio and the optimum Ni/Mn ratios are observed for 0.05:0.95 and 0.025:0.975.

In **Figure 1B**, the corresponding CO_2 conversions are shown. Similarly, $NiMn/ZrO_2$-4 and $NiMn/ZrO_2$-5 catalysts gave the best CO_2 conversion with the CO_2 conversions gradually increasing from ca. 93% to around 97% and then staying at a quasi-steady level for 10 h. It is noteworthy that the CO_2 conversions over the manganese oxide-containing catalysts experienced a gradual increase in the first hours and thereafter remained at a high and stable level. In contrast, both the CH_4 and CO_2 conversions decreased throughout the MDR reactions for the Ni/ZrO_2 catalyst. Interestingly,

although the Mn/ZrO_2 catalyst experienced a drop in CH_4 conversion, the CO_2 conversion in contrast, showed a similar trend to $NiMn/ZrO_2$ catalysts with an obvious increase at the beginning of the reactions. This we ascribe to the evolved change of oxidation states of Mn in the catalysts, as will be evidenced in our XPS studies.

In addition, as seen in **Figure 1C**, the obtained H_2/CO ratios are consistent with the CH_4 and CO_2 conversion results. The H_2/CO ratios over $NiMn/ZrO_2$-4 and $NiMn/ZrO_2$-5 fall in a very narrow range (0.997 to 0.938) which is slightly less than 1, indicating that a negligible reverse water gas shift reaction (RWGS) occurred during the microwave-assisted MDR process.[13] However, the Ni/ZrO_2 catalyst and $NiMn/ZrO_2$ catalysts with higher Ni/Mn ratio showed the H_2/CO ratios in the first several hours (normally from t= 0 to 3h) are greater than 1.

This reveals that the CH_4 cracking reaction ($CH_4 = C + 2H_2$) is more evident than carbon gasification ($C + CO_2 = 2CO$) in the early periods of reaction and consequently results in deleterious carbon deposition which subsequently degrades the methane dry reforming performances of the catalysts. Thus, a suitable Ni/Mn ratio in the prepared $NiMn/ZrO_2$ catalyst is critical in terms of resisting coke formation under microwave irradiation and it has been found that $NiMn/ZrO_2$-4 is the optimum catalyst among others for the microwave-assisted methane reforming with CO_2. We also compared this optimal catalyst with previous studies on microwave-assisted methane dry reforming (as summarised in Table S1). Notwithstanding the hot spots generated under microwave irradiation, the recorded catalyst bed temperature of $NiMn/ZrO_2$-4 in this study is much lower than that of other studies but with higher conversion of CH_4 and CO_2.

In **Figure 1D**, we present the absorbed microwave powers and catalyst bed temperatures of the representative catalysts as a function of reaction time. With a fixed microwave input power P_I at 100 W, the power of the absorbed microwaves by $NiMn/ZrO_2$-4 and Mn/ZrO_2 are in close proximity to each other and remain at a level around 48 W, whilst for Ni/ZrO_2, it decreases gradually from 72 to 29 W in 10 hours. This indicates the excellent microwave absorption

properties of the manganese oxide promoter and the microwave absorption decrease over Ni/ZrO_2 is partially attributed to the continuous carbon deposition on the Ni/ZrO_2 catalyst that reduced the dielectric properties of the sample throughout the experiment. Thus, the excellent stability of $NiMn/ZrO_2$-4 was also evidenced by the fact that no noticeable changes of its dielectric properties were observed via the stable microwave absorption during the reaction.[42]

Most importantly, the catalyst bed temperatures recorded by an IR pyrometer were normally below 220˚C, which are significantly lower than that of the traditional thermal methane dry reforming temperature (above 820 ˚C, calculated via HSC chemistry).[43] This observation once again illustrates the advantages of microwave heating in lowering overall catalyst bed temperatures for reforming methane under mild conditions. And this reduction in overall temperature would subsequently benefit the prevention of sintering of the Ni active metal to help stabilize the catalyst.

We also note of course that the generated hot spots under microwave irradiation can often be at higher temperatures than the remaining bulk support and catalyst bed. Zhang et al.[44] reported those spatial hot spots have temperatures about 100–150 °C above such surroundings which is still less than that with purely thermal activation.

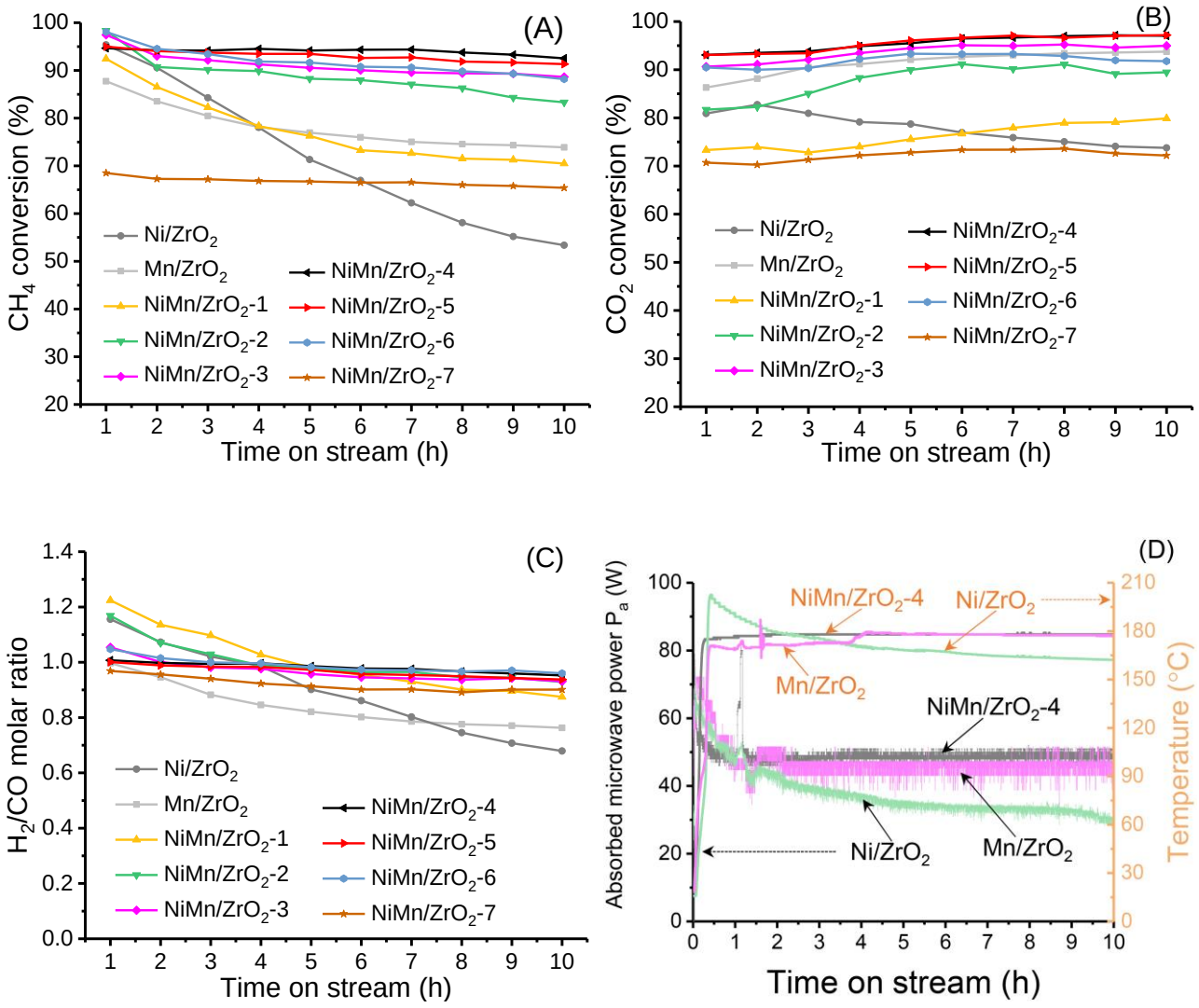


Figure 1. Experimental results of microwave-assisted methane dry reforming over different catalysts: (A) CH_4 conversion, (B) CO_2 conversion and (C) H_2/CO ratios. (D) Representative curves for the recorded microwave absorption and catalyst bed temperatures.

3.2 XRD characterization and surface morphologies

To reveal the structure changes in catalysts over the course of the reaction, X-ray diffraction patterns of the catalysts before and after MDR reactions were collected and are presented in **Figure 2**. In addition to peaks due to the monoclinic phase of the ZrO_2 support (ICDD PDF No. 07-0343), three significant diffraction peaks for NiO at 37.4˚, 43.5˚ and 63.2˚ (ICDD PDF No. 01-1239) appeared in the fresh Ni/ZrO_2 catalyst. In the fresh Mn/ZrO_2 and $NiMn/ZrO_2$-4 catalysts, the newly emerged peaks at 18.0˚, 32.7˚ and 36.2˚ (ICDD PDF No. 06-0540) are assigned to Mn_2O_3

(manganese(III) oxide). There is no observable difference between these two samples and the diminished nickel diffraction peaks in the fresh NiMn/ZrO_2-4 are due to the high dispersion or low content of nickel species in the catalyst framework.

After 10 hour-time-on-stream operation of methane reforming with CO_2, the catalysts have been transformed and significant changes between the fresh and used catalysts can be observed. In the used Ni/ZrO_2 catalyst, NiO diffraction peaks disappeared and the nickel was reduced to metallic Ni (peaks at 44.5˚, 51.8˚ and 76.4˚, ICDD PDF No. 04-0850). It is noteworthy that the used Ni/ZrO_2 also shows an obvious carbon diffraction peak at 26.2˚ compared with other samples.[13] This peak further confirms the heavy carbon deposition on Ni/ZrO_2 catalyst. In the used Mn/ZrO_2 and NiMn/ZrO_2-4 catalysts, the Mn_2O_3 has been reduced to MnO (manganosite, ICDD PDF No. 07-0230). Interestingly, a cubic phase of ZrO_2 (ICDD PDF No. 07-0337) was detected in all the used catalysts and the peak intensity observed on used NiMn/ZrO_2-4 are much stronger than that of used Ni/ZrO_2 and Mn/ZrO_2 catalysts.

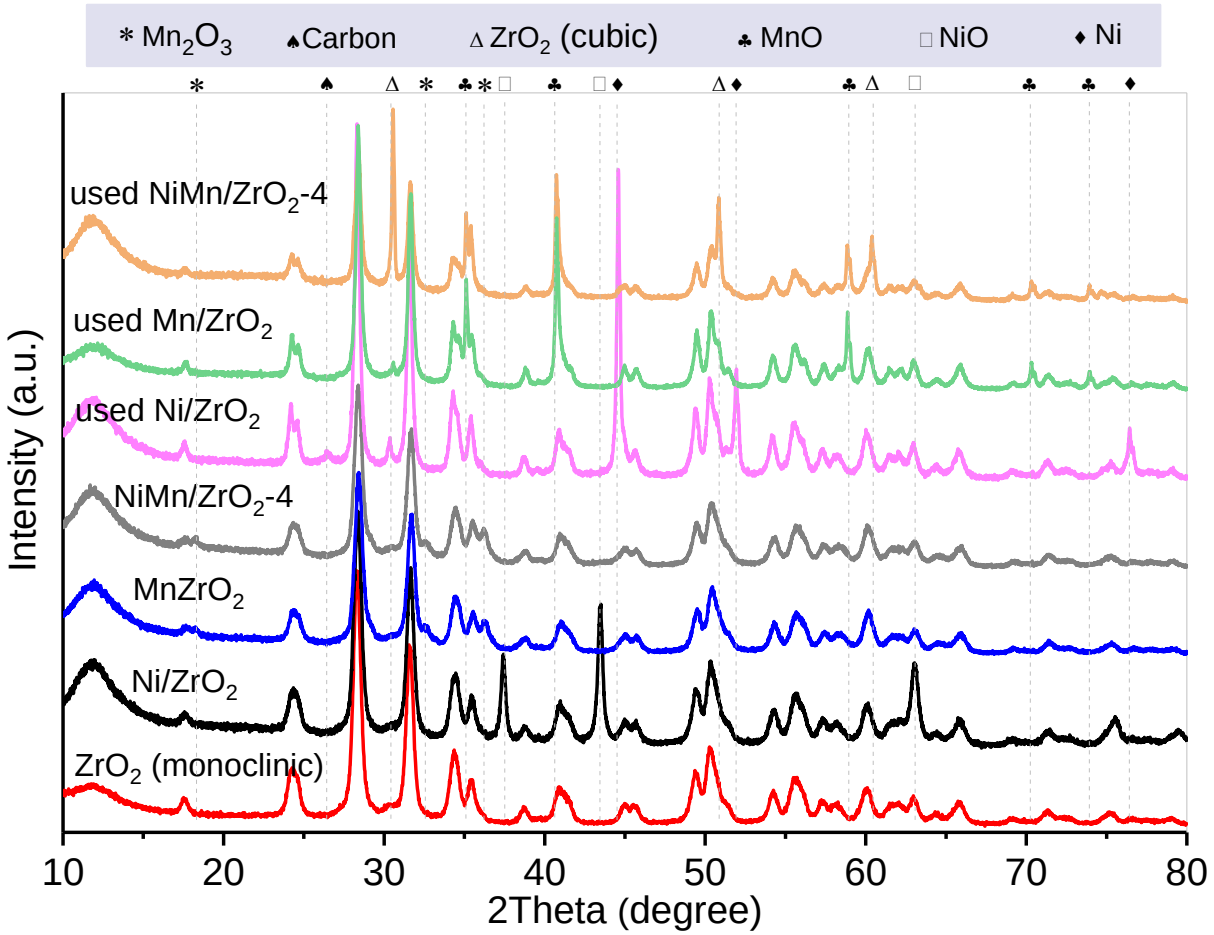
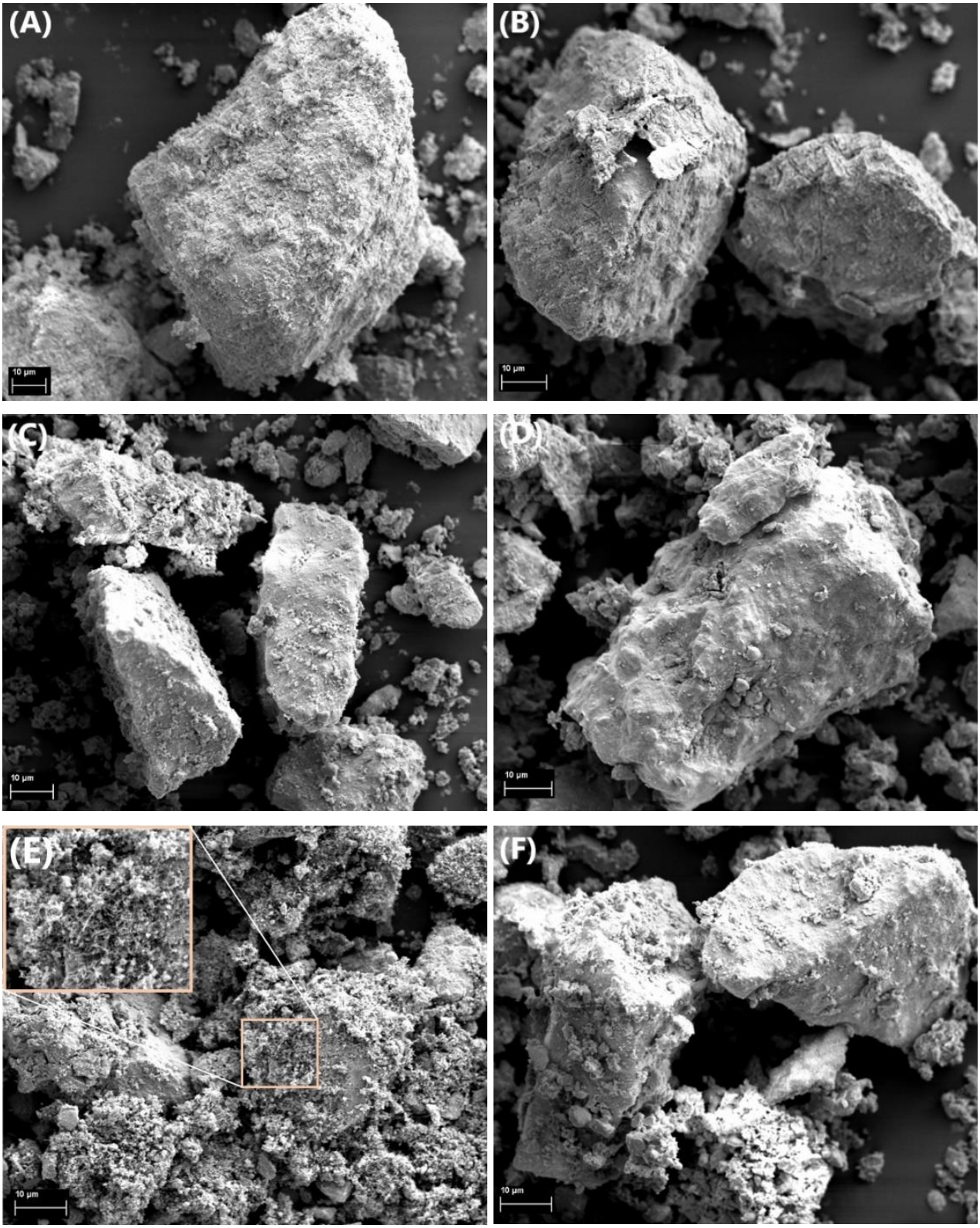


Figure 2. XRD patterns of the representative samples.

Further characterization by SEM-EDS revealed the surface morphologies of Ni/ZrO_2, Mn/ZrO_2 and $NiMn/ZrO_2$-4 catalysts both before and after the MDR reaction under microwave irradiation (**Figure 3**). It is obvious that the fresh Ni/ZrO_2, Mn/ZrO_2 and $NiMn/ZrO_2$-4 catalysts have clean surfaces, which show no inherent differences with that of the ZrO_2 support (**Figure 3A-D**,). A clear and obvious amount of carbon was found deposited on the used Ni/ZrO_2 catalyst after 10 hours MDR reaction under microwave irradiation (**Figure 3E**), whilst no noticeable changes were observed in the used Mn/ZrO_2 and $NiMn/ZrO_2$-4 catalysts (**Figure 3F** and **G**). Thus, we attribute the decreased MDR activity of Ni/ZrO_2 catalyst to the formation of filamentous carbons (inset in **Figure 3E**) that covered the nickel active sites and weakened carbon elimination.[13] The surface elemental mapping was conducted by EDS to give a semi-quantitative analysis of the fresh and used catalysts (**Figure 3H**). Compared with the fresh Ni/ZrO_2 catalyst, the surface carbon concentration

in the used Ni/ZrO_2 significantly reached 39.9 wt.%, whilst only 9.7 and 3.4 wt.% of carbon were detected on used Mn/ZrO_2 and $NiMn/ZrO_2$-4, respectively. In a brief summary, the excellent anti-coking ability of $NiMn/ZrO_2$-4 is evidenced in our pre- and post-reaction characterisation.



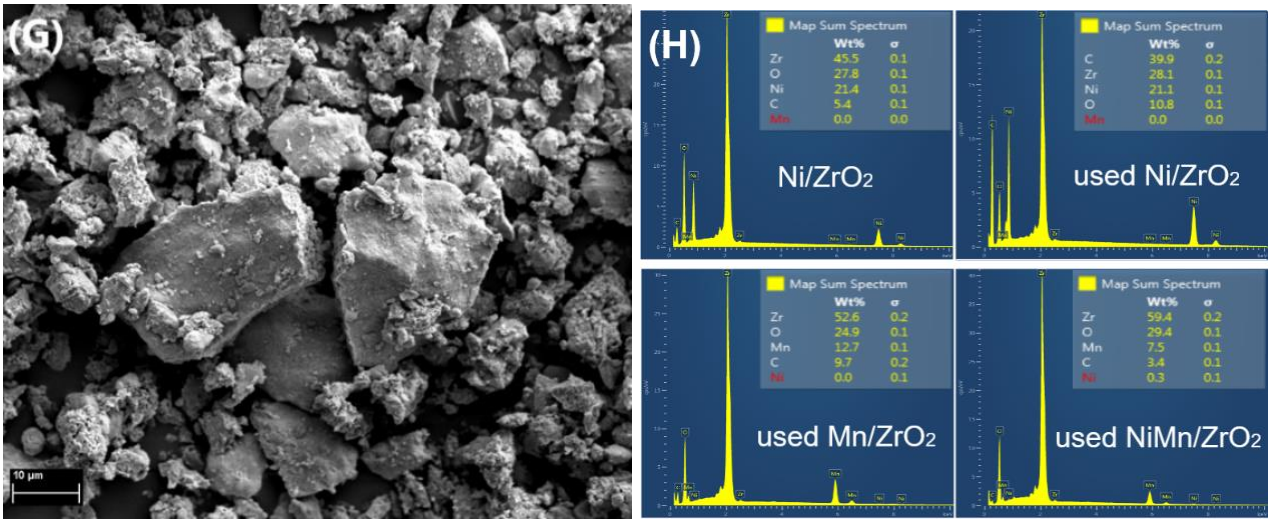


Figure 3. Morphologies and EDS analysis of the representative samples. (A) ZrO_2 supporting material. Fresh samples of (B) Ni/ZrO_2, (C) Mn/ZrO_2, and(D) NiMn/ZrO_2-4. And used samples of (E) Ni/ZrO_2, (F) Mn/ZrO_2, and (G) NiMn/ZrO_2-4. (H) EDS results.

3.3 Identification and quantification of the deposited carbon

In order to quantify precisely the content of carbon contained in the samples, thermogravimetric analysis was carried out (**Figure 4**). It is clear that the weight loss curves of ZrO_2 support and the fresh catalysts are relatively flat and very similar to each other, and these curves only show a small weight loss peak (below 100 ˚C) which is attributed to the moisture absorbed in the samples.[45] Importantly, this demonstrated that no carbon is presented in the fresh catalysts even though citric acid (obviously a potential carbon source) was used in the preparation process. Thus, it also confirms that the carbon weight losses in the used catalysts are completely attributable to carbon deposition during the MDR reaction. It can be seen that negligible carbon was observed on the used manganese oxide containing catalysts (NiMn/ZrO_2-4 and Mn/ZrO_2), and the weight gain of the used Mn/ZrO_2 and NiMn/ZrO_2-4 in the range of 200-500 °C should be originated from the re-oxidation of reduced species, such as metallic Ni or MnO.

This once again highlights the important effect of manganese oxide in terms of improving the anti-

coking ability of Ni-based catalysts. In contrast, the corresponding weight loss of carbon over the used Ni/ZrO_2 catalyst was 7.2 wt%, indicating severe carbon deposition during the MRD under microwave irradiation and the lack of coking-resistant ability for a solely Ni-based catalyst.

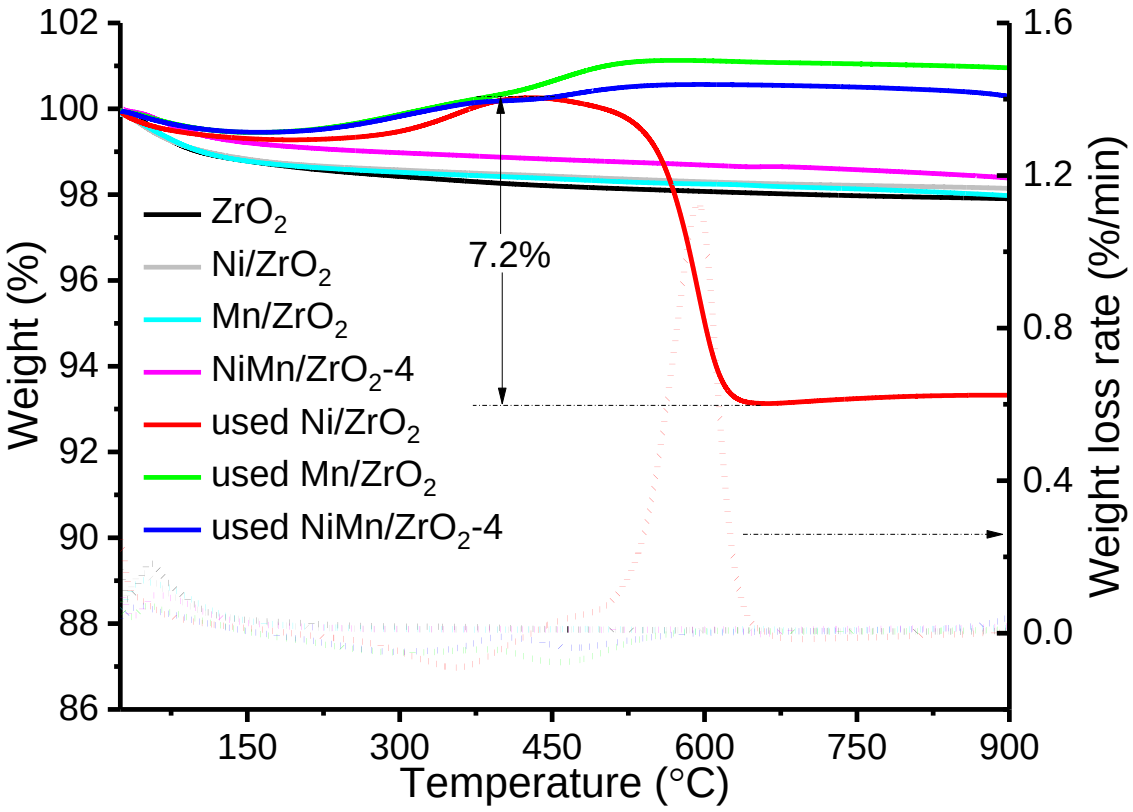


Figure 4. TGA analysis results of the pre- and post-reaction samples.

3.4 Evolved chemical states of Mn and Ni for the microwave-assisted MDR

The chemical states of Mn, Ni and O in the $NiMn/ZrO_2$, Ni/ZrO_2 and Mn/ZrO_2 catalysts were carefully studied by X-ray photoelectron spectra (XPS) before and after the methane dry reforming reaction with CO_2 under microwave irradiation. The $Mn2p_{3/2}$ peak in **Figure 5A** could be deconvoluted into three peaks with a binding energy of 640.5, 642.1 and 644.1 eV which are assigned to the Mn^{2+}, Mn^{3+} and Mn^{4+},[46,47] respectively. In the fresh catalysts, the Mn^{2+} species consisted of 13.5% and 10.9 % in $NiMn/ZrO_2$-4 and Mn/ZrO_2, respectively, whilst the Mn^{2+} concentration in the used samples was found to significantly increase to 41.3% and 49.5%. The corresponding contents of Mn^{3+} were found to drastically decrease from around 82% in the fresh

catalysts to only half, e.g. ca. 40% in both used catalysts. Clearly, a substantial higher oxidation state Mn^{3+} was reduced to Mn^{2+} throughout the MDR reaction under microwave irradiation. Previous literature[16,48] studies reported that the addition of MnO on Fe/Silicalite-2 or Ni/Al_2O_3 catalysts can enhance the capacity and the strength of CO_2 absorption and consequently increase the reactivity of CO_2. We therefore attribute the increasing CO_2 conversion that observed at the initial several hours of reactions (**Figure 1B**) to the result of evolved chemical state changes of manganese in $NiMn/ZrO_2$ catalysts where more Mn^{2+} was present, thus enhancing the CO_2 absorption and resulting consumption. It should be also noted that a desired ratio of Mn^{3+}/Mn^{2+} was naturally adjusted when the reactions started and subsequently achieved a balance between the different oxidation states of manganese oxide.

In **Figure 5B** we present the Ni2p narrow scan spectra of the fresh and used catalysts. The positions with binding energies of 852.9, 854.1 and 856.3 eV correspond to the metallic Ni, NiO and NiOOH, respectively.[49-52] Compared with the fresh catalysts where no metallic Ni was detected, a noticeable peak assigned to metallic Ni appeared in the used catalysts, confirming the presence of metallic Ni species during the reforming reaction. We also note that, under the same characterization conditions, the Ni2p intensity in the Ni/ZrO_2 catalyst significantly decreased after reaction. This is ascribed to the heavy carbon deposition on the used Ni/ZrO_2 catalyst which have also been confirmed in our XRD, TGA and SEM-EDS analysis,[53,54] and consequently resulting in loss of nickel sites for the CO_2 and methane reforming reaction.[13] In contrast, both the used and fresh $NiMn/ZrO_2$-4 catalysts show similar Ni2p intensities, again reflecting the negligible carbon deposition on manganese oxide-modified nickel catalyst.

As seen in **Figure 5C**, the O1s spectra could be deconvoluted into two peaks centered in the narrow ranges of 529.4-529.8 eV and 531.0-531.5 eV, and these two peaks are assigned to the surface lattice oxygen and the oxide surface phase composed of ZrO_2, respectively.[55,56] As a general observation, both the intensity of O1s spectra and the concentration of surface lattice oxygen peak

decreased after the methane reforming with CO_2. For the Ni/ZrO_2 catalyst, the concentration of surface lattice oxygen species drastically dropped from 69.8% in the fresh catalyst to ca.18.7% after the supported nickel oxide being reduced into metallic state. While, the surface lattice oxygen concentrations in the used manganese oxide-containing catalysts ($NiMn/ZrO_2$-4 and Mn/ZrO_2) are kept at high levels of 45.9% and 60%, respectively, and both of these two concentrations are still around 70% of the initial concentration in their corresponding fresh catalyst. This reveals that the manganese oxide promoter could help the catalysts to preserve surface lattice oxygen at a high and stable level because of the formation of Mn^{3+}/Mn^{2+} redox couple during the reforming reaction.[57] Thus, the preserved and abundant surface lattice oxygen could work as active oxygen species to eliminate the deposited coke on catalyst as CO [58,59] and provide improved coking-resistant ability to the nickel-based catalysts.

It is clear that the manganese oxide-promoted nickel catalyst supported over ZrO_2 for the carbon dioxide reforming of methane stabilizes the catalytic activity by suppressing the formation of carbon deposits on the metal catalyst particles. The evolved reduction of Mn^{3+} to Mn^{2+} is considered to be beneficial for the absorption and conversion of CO_2 and the formed Mn^{3+}/ Mn^{2+} redox couple could help the catalyst to preserve active oxygen species at a stable and high concentration. This would significantly release the metallic nickel active sites for the methane activation whilst also enhance the molecular kinetics for the gasification of carbons and consequently inhibiting the carbon deposition. Furthermore, the significantly suppressed carbon deposition on the manganese oxide modified nickel-based samples will stabilize the catalyst to achieve stable microwave energy conversion and methane reforming.

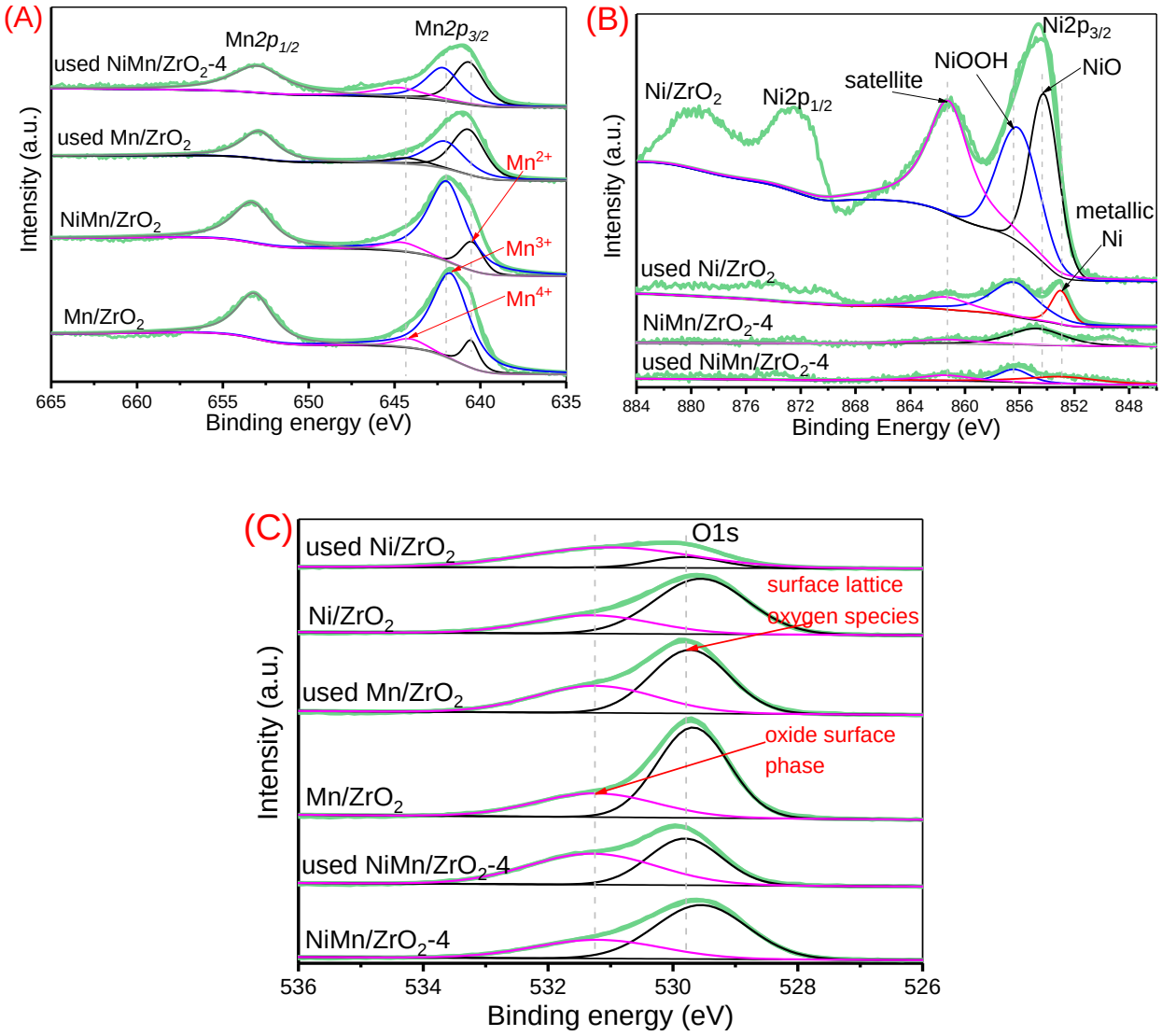


Figure 5. Narrow XPS scan spectra: (A) Mn2p spectra, (B) Ni2p spectra and (C) O1s spectra.

4. Concluding Remarks

Manganese oxide-modified nickel-based catalysts supported over ZrO_2 were synthesized and tested for CO_2 reforming of methane to generate syngas under non-thermal, microwave-initiated conditions. The performance of the nickel catalysts with and without manganese oxide modification were thoroughly investigated. Under microwave-initiation, the Ni/ZrO_2 catalyst (without manganese oxide modification) showed stronger methane cracking than carbon gasification in the initial reaction stage, consequently resulting in severe filamentous carbon deposition. The carbon deposition not only causes the blockage of nickel active sites but also changed the dielectric

properties that consequently weakened microwave absorption. With the addition of manganese oxide, the nickel catalyst achieved very stable MDR performance under mild conditions with both CH_4 and CO_2 conversions being above 93% and the product H_2/CO ratio falling in a stoichiometric range of 0.997~0.938.

Importantly, the presence of manganese oxide in the catalysts helps suppress carbon deposition, as the evolved reduction of Mn^{3+} to Mn^{2+} is favourable for both CO_2 absorption and accompanying conversion and enhances the gasification of carbons thus inhibiting the carbon deposition. This work reveals the importance of manganese oxide promoter in improving the anti-coke ability of nickel-based catalyst for microwave-assisted methane dry reforming process. Furthermore, the interaction between Ni catalysts (with and without manganese oxide) and the incident microwave electric field is presented as a guiding principle for enhancing a catalytic systems performance.

Acknowledgement

The authors would like to acknowledge the financial support from EPSRC. And we thank Dr Shaoliang Guan at Harwellxps for conducting X-ray photoelectron spectroscopy analysis. Weisong Li and Xiangyu Jie are also grateful to the China Scholarship Council (CSC) for scholarships.

Reference

1. International Energy Agency (IEA). *Global Energy & CO_2 Status Report*. **2017**.
2. Tian, S.; Yan, F.; Zhang, Z.; Jiang, J. Calcium-looping reforming of methane realizes in situ CO_2 utilization with improved energy efficiency. *Sci. Adv.* **2019**, *5*, eaav5077.
3. Rogelj, J.; Den Elzen, M.; Höhne, N.; Fransen, T.; Fekete, H.; Winkler, H.; Schaeffer, R.; Sha, F.; Riahi, K.; Meinshausen, M. Paris Agreement climate proposals need a boost to keep warming well below 2 ˚C. *Nature.* **2016**, *534*, 631-639.
4. Jie, X.; Gonzalez-Cortes, S.; Xiao, T.; Yao, B.; Wang, J.; Slocombe, D. R.; Thomas, J. M.; Edwards, P. P. The decarbonisation of petroleum and other fossil hydrocarbon fuels for the

facile production and safe storage of hydrogen. *Energ. Environ. Sci.* **2019**, *12*, 238-249.

5. Peter, S. C. Reduction of CO_2 to Chemicals and Fuels: A Solution to Global Warming and Energy Crisis. *ACS Energ. Lett.* **2018**, *3*, 1557-1561.
6. Numpilai, T.; Witoon, T.; Chanlek, N.; Limphirat, W.; Bonura, G.; Chareonpanich, M.; Limtrakul, J. Structure–activity relationships of Fe-Co/K-Al_2O_3 catalysts calcined at different temperatures for CO_2 hydrogenation to light olefins. *Appl. Catal. A: Gen.* **2017**, *547*, 219-229.
7. Wang, L.; Wang, L.; Zhang, J.; Liu, X.; Wang, H.; Zhang, W.; Yang, Q.; Ma, J.; Dong, X.; Yoo, S. J.; Kim, J. G.; Meng X. J.; Xiao, F. S. Selective hydrogenation of CO_2 to ethanol over cobalt catalysts. *Angew. Chem. Int. Edit.* **2018**, *57*, 6104-6108.
8. Tu, W.; Zhou, Y.; Zou, Z. Photocatalytic conversion of CO_2 into renewable hydrocarbon fuels: state-of-the-art accomplishment, challenges, and prospects. *Adv. Mater.* **2014**, *26*, 4607-4626.
9. Whipple, D. T.; Kenis, P. J. Prospects of CO_2 utilization via direct heterogeneous electrochemical reduction. *J. Phys. Chem. Lett*. **2010**, *1*, 3451-3458.
10. Zhang, C.; Yang, S.; Wu, J.; Liu, M.; Yazdi, S.; Ren, M.; Li, Z. Electrochemical CO_2 Reduction with Atomic Iron-Dispersed on Nitrogen-Doped Graphene. *Adv. Energ. Mater.* **2018**, *8*, 1703487.
11. Liu, C. J.; Ye, J.; Jiang, J.; Pan, Y. Progresses in the preparation of coke resistant Ni-based catalyst for steam and CO_2 reforming of methane. *ChemCatChem*. **2011**, *3*, 529-541.
12. Sun, N.; Wen, X.; Wang, F.; Wei, W.; Sun, Y. Effect of pore structure on Ni catalyst for CO_2 reforming of CH_4. *Energ. Environ. Sci.*, **2010**, *3*, 366-369.
13. Wang, C.; Jie, X.; Qiu, Y.; Zhao, Y.; Al-Megren, H. A.; Alshihri, S.; Xiao, T. The importance of inner cavity space within Ni@ SiO_2 nanocapsule catalysts for excellent coking resistance in the high-space-velocity dry reforming of methane. *Appl. Catal. B: Environ.* **2019**, *259*, 118019.
14. Ma, H.; Zeng, L.; Tian, H.; Li, D.; Wang, X.; Li, X.; Gong, J. Efficient hydrogen production from ethanol steam reforming over La-modified ordered mesoporous Ni-based catalysts. *Appl.*

Catal. B: Environ. **2016**, *181*, 321-331.

15. Seok, S. H.; Choi, S. H.; Park, E. D.; Han, S. H.; Lee, J. S. Mn-promoted Ni/Al_2O_3 catalysts for stable carbon dioxide reforming of methane. *J. Catal.* **2002**, *209*, 6-15.
16. Seok, S. H.; Han, S. H.; Lee, J. S. The role of MnO in $Ni/MnO\text{-}Al_2O_3$ catalysts for carbon dioxide reforming of methane. *Appl. Catal. A: Gen.* **2001**, *215*, 31-38.
17. Yao, L.; Shi, J.; Hu, C. The structure, carbon deposition and stability of a $ZrO_x/Ni–MnO_x/SiO_2$ catalyst for the CO_2 reforming of methane. *RSC Adv.* **2015**, *5*, 90168-90177.
18. Zhu, J.; Peng, X.; Yao, L.; Tong, D.; Hu C. CO_2 reforming of methane over Mg-promoted Ni/SiO_2 catalysts: the influence of Mg precursors and impregnation sequences. *Catal. Sci. Technol.* **2012**, *2*, 529-537.
19. Guo, M.; Lu, G. The effect of impregnation strategy on structural characters and CO_2 methanation properties over MgO modified Ni/SiO_2 catalysts. *Catal. Commun.* **2014**, *54*, 55-60.
20. Gonzalez-Cortes, S.; Slocombe, D. R.; Xiao, T.; Aldawsari, A.; Yao, B.; Kuznetsov, V. L.; Thomas, J. M.; Edwards, P. P. Wax: A benign hydrogen-storage material that rapidly releases H_2-rich gases through microwave-assisted catalytic decomposition. *Sci. Rep.* **2016**, *6*, 35315.
21. de la Hoz, A.; Diaz-Ortiz, A.; Moreno, A.; Microwaves in organic synthesis. Thermal and non-thermal microwave effects. *Chem. Soc. Rev.* **2005**, *34*, 164-178.
22. Zhang, X.; Hayward, D. O.; Lee, C.; Mingos, D. M. P.; Microwave assisted catalytic reduction of sulfur dioxide with methane over MoS_2 catalysts. *Appl. Catal. B: Environ.* **2001**, *33*, 137-148.
23. Pizzetti, M.; Petricci, E.; Tecnologico, C.; Heterogeneous catalysis under microwave heating. *La Chimica & L'Industria*, **2012**, *12*, 78-81.
24. Zhang, X.; Lee, C. S. M.; Mingos, D. M. P.; Hayward, D. O.; Carbon dioxide reforming of methane with Pt catalysts using microwave dielectric heating. *Catal. Lett.* **2003**, *88*, 129-139.
25. Domínguez, A.; Fernández, Y.; Fidalgo, B.; Pis, J. J.; Menéndez, J. A. Biogas to syngas by microwave-assisted dry reforming in the presence of char. *Energ. Fuel.* **2007**, *21*, 2066-2071.

26. Zhang, F.; Song, Z.; Zhu, J.; Liu, L.; Sun, J.; Zhao, X.; Wang, W. Process of CH_4-CO_2 reforming over Fe/SiC catalyst under microwave irradiation. *Sci. Total Environ.* **2018**, *639*, 1148-1155.
27. Odedairo, T.; Ma, J.; Chen, J.; Zhu, Z. Cr-Doped La-Ni-O Catalysts Derived from Perovskite Precursors for CH_4-CO_2 Reforming under Microwave Irradiation. *Chem. Eng. Tech.* **2016**, *39*, 1551-1560.
28. Gangurde, L. S.; Sturm, G. S.; Valero-Romero, M. J.; Mallada, R.; Santamaria, J.; Stankiewicz, A. I.; Stefanidis, G. D. Synthesis, characterization, and application of ruthenium-doped $SrTiO_3$ perovskite catalysts for microwave-assisted methane dry reforming. *Chem. Eng. Process.* **2018**, *127*, 178-190.
29. Wang, C.; Sun, N.; Zhao, N.; Wei, W.; Sun, Y.; Sun, C.; Snape, C. E. Coking and deactivation of a mesoporous Ni–CaO–ZrO_2 catalyst in dry reforming of methane: a study under different feeding compositions. *Fuel.* **2015**, *143*, 527-535.
30. Huang, X.; Xue, G.; Wang, C.; Zhao, N.; Sun, N.; Wei, W.; Sun, Y. Highly stable mesoporous NiO–Y_2O_3–Al_2O_3 catalysts for CO_2 reforming of methane: effect of Ni embedding and Y_2O_3 promotion. *Catal. Sci. Technol.* **2016**, *6*, 449-459.
31. Wang, N.; Shen, K.; Huang, L.; Yu, X.; Qian, W.; Chu, W. Facile route for synthesizing ordered mesoporous Ni–Ce–Al oxide materials and their catalytic performance for methane dry reforming to hydrogen and syngas. *ACS Catal.* **2013**, *3*, 1638-1651.
32. Li, Z.; Mo, L.; Kathiraser, Y.; Kawi, S. Yolk–satellite–shell structured Ni–yolk@ Ni@SiO_2 nanocomposite: superb catalyst toward methane CO_2 reforming reaction. *ACS Catal.* **2014**, *4*, 1526-1536.
33. Fidalgo, B.; Arenillas, A.; Menéndez, J. Á. Synergetic effect of a mixture of activated carbon+Ni/Al_2O_3 used as catalysts for the CO_2 reforming of CH_4. *Appl. Catal. A: Gen.* **2010**, *390*, 78-83.

34. Li, L.; Jiang, X.; Wang, H.; Wang, J.; Song, Z.; Zhao, X.; Ma, C. Methane dry and mixed reforming on the mixture of bio-char and nickel-based catalyst with microwave assistance. *J. Anal. Appl. Pyrol.* **2017**, *125*, 318-327.
35. Fidalgo, B.; Zubizarreta, L.; Bermúdez, J. M.; Arenillas, A.; Menéndez, J. A.; Synthesis of carbon-supported nickel catalysts for the dry reforming of CH_4. *Fuel Process. Tech.* **2010**, *91*, 765-769.
36. Littlewood, P.; Xie, X.; Bernicke, M.; Thomas, A.; Schomäcker, R. $Ni_{0.05}Mn_{0.95}O$ catalysts for the dry reforming of methane. *Catal. Today*. **2015**, *242*, 111-118.
37. Wang, P.; Zhao, G.; Wang, Y.; Lu, Y. $MnTiO_3$-driven low-temperature oxidative coupling of methane over TiO_2-doped Mn_2O_3-Na_2WO_4/SiO_2 catalyst. *Sci. Adv.* **2017**, *3*, e1603180.
38. Rawat, K. S.; Mahata, A.; Choudhuri, I.; Pathak, B. Catalytic hydrogenation of CO_2 by manganese complexes: role of π-acceptor ligands. *J. Phys. Chem. C*. **2016**, *120*, 16478-16488.
39. Altantuya, O.; Sápi, A.; Kukovecz, Á.; Kónya, Z. One-pot mechanochemical synthesis of Cu and Pt-doped MnO_x nanostructures as efficient catalysts in CO_2 hydrogenation reaction; Manganese-balance drives activity. *Appl. Cata. A-Gen.* **2019**.
40. Chang, T.; Shen, Z.; Huang, Y.; Lu, J.; Ren, D.; Sun, J.; Liu, H. Post-plasma-catalytic removal of toluene using MnO_2–Co_3O_4 catalysts and their synergistic mechanism. *Chem. Eng. J.* **2018**, *348*, 15-25.
41. Yao, L.; Galvez, M. E.; Hu, C.; Da Costa, P.; Synthesis Gas Production via Dry Reforming of Methane over Manganese Promoted Nickel/Cerium–Zirconium Oxide Catalyst. *Ind. Eng. Chem. Res.* **2018**, *57*, 16645-16656.
42. Liu, B.; Slocombe, D. R.; Wang, J.; Aldawsari, A.; Gonzalez-Cortes, S.; Arden, J.; Edwards, P. P. Microwaves effectively examine the extent and type of coking over acid zeolite catalysts. *Nat. commun*. **2017**, *8*, 514.
43. Pakhare, D.; Spivey, J. A review of dry (CO_2) reforming of methane over noble metal

catalysts. *Chem. Soc. Rev.* **2014**, *43*, 7813-7837.

44. Zhang, X.; Hayward, D. O.; Mingos, D. M. P. Effects of microwave dielectric heating on heterogeneous catalysis. *Catal. Lett.* **2003**, *88*, 33-38.
45. Al-Fatesh, A.; Singh, S. K.; Kanade, G. S.; Atia, H.; Fakeeha, A. H.; Ibrahim, A. A.; Labhasetwar, N. K. Rh promoted and ZrO_2/Al_2O_3 supported Ni/Co based catalysts: High activity for CO_2 reforming, steam–CO_2 reforming and oxy–CO_2 reforming of CH_4. *Int. J. Hydro. Energ.* **2018**, *43*, 12069-12080.
46. Di Castro, V.; Polzonetti, G. XPS study of MnO oxidation. *J. Electron Spectrosc.* **1989**, *48*, 117-123.
47. Liu, A.; Lv, Y.; Mu, J.; Guo, Z.; Pei, Z.; Zhang, X.; Che, H. Facile synthesis of hollow $Ni_{0.2}Mn_{0.8}O_{1.5}$ twin microspheres for electrochemical energy storage. *J. Appl. Electro.* **2018**, *48*, 15-26.
48. Xu, L.; Wang, Q.; Liang, D.; Wang, X.; Lin, L.; Cui, W.; Xu, Y. The promotions of MnO and K_2O to Fe/silicalite-2 catalyst for the production of light alkenes from CO_2 hydrogenation. *Appl. Catal. A: Gen.* **1998**, *173*, 19-25.
49. Park, K. W.; Choi, J. H.; Kwon, B. K.; Lee, S. A.; Sung, Y. E.; Ha, H. Y.; Wieckowski, A. Chemical and electronic effects of Ni in Pt/Ni and Pt/Ru/Ni alloy nanoparticles in methanol electrooxidation. *J. Phys. Chem. B*. **2002**, *106*, 1869-1877.
50. Luo, P. F.; Kuwana, T.; Paul, D. K.; Sherwood, P. M. Electrochemical and XPS study of the nickel−titanium electrode surface. *Anal. Chem.* **1996**, *68*, 3330-3337.
51. Ng, K. T.; Hercules, D. M. Studies of nickel-tungsten-alumina catalysts by X-ray photoelectron spectroscopy. *J. Phys. Chem.* **1976**, *80*, 2094-2102.
52. Liang, Y.; Paul, D. K.; Xie, Y.; Sherwood, P. M. Core and valence band photoelectron spectroscopic studies of nickel oxidation in an anaerobic liquid cell. *Anal. Chem.* **1993**, *65*, 2276-2281.

53. Vissers, J. P. R.; Mercx, F. P. M.; Bouwens, S. M. A. M.; De Beer, V. H. J.; Prins, R. Carbon-covered alumina as a support for sulfide catalysts. *J. Catal.* **1988**, *114*, 291-302.

54. Oultache, A. K.; Prud'homme, R. E. XPS studies of Ni deposition on polymethyl methacrylate and poly (styrene-co-acrylonitrile). *Polym. Advan. Technol.* **2000**, *11*, 316-323.

55. Jiang, X.; Li, X.; Wang, J.; Long, D.; Ling, L.; Qiao, W. Three-dimensional Mn–Cu–Ce ternary mixed oxide networks prepared by polymer-assisted deposition for HCHO catalytic oxidation. *Catal. Sci. Technol.* **2018**, *8*, 2740-2749.

56. Wang, C.; Sun, N.; Wei, W.; Zhao, Y. Carbon intermediates during CO_2 reforming of methane over $NiCaOZrO_2$ catalysts: A temperature-programmed surface reaction study. *Int. J. Hydro. Energ.* **2016**, *41*, 19014-19024.

57. Gandhe, A. R.; Rebello, J. S.; Figueiredo, J. L.; Fernandes, J. B. Manganese oxide OMS-2 as an effective catalyst for total oxidation of ethyl acetate. *Appl. Catal. B: Environ.* **2007**, *72*, 129-135.

58. Mukai, D.; Tochiya, S.; Murai, Y.; Imori, M.; Hashimoto, T.; Sugiura, Y.; Sekine, Y. Role of support lattice oxygen on steam reforming of toluene for hydrogen production over $Ni/La_{0.7}Sr_{0.3}AlO_{3-\delta}$ catalyst. *Appl. Catal. A: Gen.* **2013**, *453*, 60-70.

59. Wang, N.; Chu, W.; Zhang, T.; Zhao, X. S. Manganese promoting effects on the $Co–Ce–Zr–O_x$ nano catalysts for methane dry reforming with carbon dioxide to hydrogen and carbon monoxide. *Chem. Eng. J.* **2011**,*170*, 457-463.